X-ray standing wave study of Si clusters on a decagonal Al-Co-Ni quasicrystal surface

D. P. Woodruff,[1] J. Ledieu,[2] K. R. J. Lovelock,[3] Robert G. Jones,[3] A. Deyko,[3] L. H. Wearing,[4] R. McGrath,[4] A. Chaudhuri,[1] H. I. Li,[5] S. Y. Su,[5] A. Mayer,[5] N. A. Stanisha,[5] and R. D. Diehl[5]

[1]*Department of Physics, University of Warwick, Coventry, CV4 7AL, United Kingdom*

[2]*Institut Jean Lamour UMR7198 (CNRS-Université de Lorraine), Parc de Saurupt, 54011 Nancy Cedex, France*

[3]*School of Chemistry, University of Nottingham, Nottingham, NG7 2RD, United Kingdom*

[4]*Department of Physics and Surface Science Research Centre, University of Liverpool, Liverpool, L69 3BX, United Kingdom*

[5]*Department of Physics, Penn State University, University Park, Pennsylvania 16802, USA*

(Received 19 December 2014; revised manuscript received 23 February 2015; published 12 March 2015)

Quantitative adsorption structure determinations on quasicrystals are scarce because most techniques for measuring surface structures are not well suited to the complex and infinite unit cells of quasicrystals. The normal incidence standing x-ray wave field technique presents a solution to these problems because it can be made inherently surface sensitive and does not involve extensive computational effort. We describe a method for applying this technique to adsorbates on quasicrystals, with specific application to a submonolayer of Si atoms on a decagonal Al-Co-Ni surface. We demonstrate the sensitivity of the technique to both adsorption site and geometry, leading to the conclusion that the Si atoms, which form six-atom pentagonal clusters, have an average height of 1.77 ± 0.05 Å above pentagonal hollow sites, with a significant height variation among the Si atoms in the cluster. In particular, the central Si atom sits more deeply than the five surrounding Si atoms, which are, on average, 2.7 Å away from the central Si atom. Although this study was performed on a decagonal quasicrystal that is periodic perpendicular to the surface, we describe how the technique can be applied to cases with no periodicity.

DOI: 10.1103/PhysRevB.91.115418 PACS number(s): 68.43.Fg, 68.49.Uv, 61.44.Br, 68.35.bd

I. INTRODUCTION

Quasicrystals are crystalline materials that have aperiodic order rather than the periodic order associated with most crystals. This aperiodic order leads to intriguing physical properties [1,2]. Although many of the well-studied quasicrystals are metal alloys, they have low electrical and thermal conductivity. They also have unusual surface properties, such as unusually low coefficients of friction and low surface energies. Because of these unusual properties, there has been an interest in the growth of quasicrystalline arrays or films on the surfaces of quasicrystals, particularly those comprising a single element. Many examples of films or arrays having some degree of quasicrystalline order have been identified, but despite the intense study for the past 25 years, few quantitative structures have been determined. The probable reason for this paucity of structural information is that the most quantitative surface structural techniques are ill suited to investigate aperiodic structures. However, many of the special properties attributed to quasicrystal surfaces such as high hardness, wear resistance, reduced friction, and nonwetting are a consequence of their aperiodic structures, so quantitative structural information is important.

An area of particular interest is the possibility to provide an aperiodic template for molecular ordering [3], with a view towards producing molecular materials with specific properties that cannot be achieved in periodic structures and that might be useful in optical circuits [4] or as catalysts [5]. It has been demonstrated that overlayer quasiperiodic arrangements of molecules or clusters can be achieved in a few cases [3,6–9]. Imaging techniques are essential in these studies for identifying characteristics such as nucleation, growth, and size, shape, and orientation of clusters or molecules, and in the absence of other methods, scanning tunneling microscopy (STM) has been used also in conjunction with density functional theory (DFT) to obtain some quantitative information related to the atomic structures of clusters and overlayers [6,10]. However, additional experimental methods are necessary to gain a more complete understanding of these structures.

Low-energy electron diffraction (LEED) is the most widely exploited surface structural technique for obtaining quantitative information related to adsorption geometry. It requires computationally demanding multiple-scattering calculations that grow rapidly with increasing size of the surface unit mesh. Although advances in computers have steadily increased the complexity of surface structures solved using LEED, quasicrystals pose an exceptional challenge because their unit cells are infinite. This requires the use of approximations, such as replacing individual atoms with average distributions [11–14] or using structure models for true periodic structures (quasicrystal approximants) that have local features similar to those in the quasicrystal [15–17]. The former approach suffers from lack of specific information about the positions of the atoms in the crystal, while the latter suffers from a limitation on the feasible size of the approximant model, which is about 65 atoms per layer in the largest approximant used so far [17]. To date, just one example of a thin film grown on a quasicrystal, that of a Cu film on the fivefold symmetric surface of icosahedral Al-Pd-Mn, has been structurally characterized with LEED [16]; this was performed using the second analysis technique described above.

Surface x-ray diffraction (SXRD) has the advantage, relative to LEED, of not requiring extensive multiple-scattering calculations, and the formalism for analyzing the crystal truncation rods for an aperiodic structure has been derived and applied to the fivefold surface of icosahedral Al-Pd-Mn [18]. This analysis was applied only to the specular truncation rod; as a consequence it was sensitive only to the average

composition and relaxation of the surface layers, and not to the atomic structure within the layers or their lateral registry. To our knowledge, this is the only quantitative SXRD study of a quasicrystal surface, and there are no examples of the application of SXRD to adsorption on a quasicrystal.

Medium-energy ion scattering (MEIS) has also been applied to obtain similar information on the relaxation and composition of the same Al-Pd-Mn surface [19]. In addition, it has been used to investigate the growth of Cu [20], Bi [21], and Fe [22] films and Au-Al alloy formation [23] on the same surface, although it has not yet been possible to obtain adsorbate geometries from MEIS studies. Similarly, x-ray photoelectron diffraction has been used to obtain information on the surface terminations of the clean surfaces of quasicrystals [24–28], but the technique is not well suited to the study of adsorbates on quasicrystals [28].

Normal-incidence x-ray standing wavefield (NISXW) is a technique aimed specifically at the quantitative study of adsorbate geometries. The general SXW method requires highly perfect crystalline samples, but the NIXSW variant can be applied to study the structures of adsorbates on surfaces of crystals that may possess some degree of mosaicity, such as most metal single crystals [29,30]. We have recently demonstrated that quantitative structural information can be obtained for adsorbed clusters on a quasicrystalline surface using NISXW [31]. Here we provide a more detailed description of this work and of the general methodology of NIXSW applied to quasicrystals.

Relative to conventional x-ray diffraction (XRD), XSW methods have the special advantage that they provide a partial solution to the "phase problem." Specifically, in XRD it is straightforward to determine the *intensities* of a large number of diffraction beams, from which one can determine their amplitude, but not their phase; as a consequence, one cannot access directly the real-space structure by a simple Fourier transformation of the experimental data. A range of methods has been developed to circumvent this problem in x-ray crystallography. In XSW, by contrast, one is only able to probe one diffraction condition in each experiment, but the information that emerges directly is both the amplitude and the phase of a single Fourier component of the structure. X-ray absorption of a single elemental species is monitored in the standing wave. In the vocabulary of XSW, each experiment at a single diffraction condition measures two parameters, the coherent fraction (CF) and the coherent position (CP). These correspond to the amplitude and phase of this single Fourier component of the structural location of the atomic species whose x-ray absorption is measured. On crystalline surfaces, NIXSW measurements allow one to determine the absolute location of adsorbate atoms relative to the underlying atomic scattering planes by measuring the spacing (equal to the CP value for a single layer spacing) of these atoms from two or more (nonparallel) sets of scattering planes. On a surface having threefold or higher symmetry, just two such measurements allow complete triangulation of the absorber site.

In quasicrystals, the existence of x-ray diffracted beams means that x-ray standing waves must be formed, and this has been demonstrated both theoretically [32,33] and experimentally [34–36]. These previous studies show that the distribution of the atoms in the quasicrystal relative to the standing wave (i.e., perpendicular to the associated scattering planes) is not random, but is grouped into limited ranges of relative position, so that NIXSW measurements of absorption at the different elemental species within the material yield nonzero values of the CF, and the results can cast light on the issue of whether or not the crystals studied have evidence of centrosymmetry [37].

A fundamental problem for NIXSW studies of surface structures is that the standing wave that is established in the bulk quasicrystal has no simple and unique phase relationship to the atoms in the surface layer; this would at first seem to render the technique useless, but in fact it only leads to some loss of precision. A second problem for the 10-fold decagonal surface studied here is the complexity of the structure: specifically, the crystal has $P\overline{1}02c$ symmetry [38,39], which has overall fivefold symmetry in the plane of the (00001) surface studied here. This structure yields 10-fold symmetric diffracted beam intensities, but the associated structure factors can be no more than fivefold symmetric. This precludes the identification of single CP and CF values using a single value of the structure factor. Nevertheless, we show how measurements of NIXSW absorption profiles can be used to determine the adsorbate locations relative to the underlying quasicrystal surface using the same general trial-and-error modeling approach that characterizes other surface structural methods.

The specific system studied here is Si adsorption on the 10-fold surface of decagonal $Al_{72}Co_{17}Ni_{11}$, the Co-rich modification of the decagonal quasicrystal, which has the 5D space group symmetry $P\overline{1}02c$ [38,39], and an atomic arrangement with the symmetry of a pentagonal prism. Thus, this quasicrystal structure consists of groups of aperiodic fivefold symmetric layers stacked in a periodic arrangement. The periodicity is described by a repeated unit comprising four alternating flat and buckled layers of atoms, with the buckling consistent with an inversion center located within a flat plane [40–42]. An earlier LEED study of the (00001) surface of this quasicrystal found that the surface is terminated by a buckled layer [15,17]. The average interlayer spacings of the surface layers were found to be the same as for the bulk structure. Here we show that NIXSW measurements from the truly periodic scattering planes parallel to the surface allow us to determine the average height of adsorbed Si atoms above the underlying surface in a standard fashion, as for a fully crystalline material. In order to determine the preferred lateral positions of the Si atoms on the surface, however, we must exploit standing waves set up in directions for which the layer spacings are aperiodic. The interpretation of these measurements led us to develop a different method for analyzing NIXSW profiles, in which we simulate profiles from model structures instead of directly fitting the profiles with single values of CP and CF.

II. EXPERIMENTAL DETAILS

The experimental procedures were described in our earlier paper [31]. Briefly, the surface of the $Al_{72}Co_{17}Ni_{11}$(00001) quasicrystal sample, originally grown at Ames Laboratory using the melt decantation method [43], was cleaned by 750 eV Ar^+ ion bombardment, followed by annealing at 800 °C (for more than 30 h), resulting in the expected

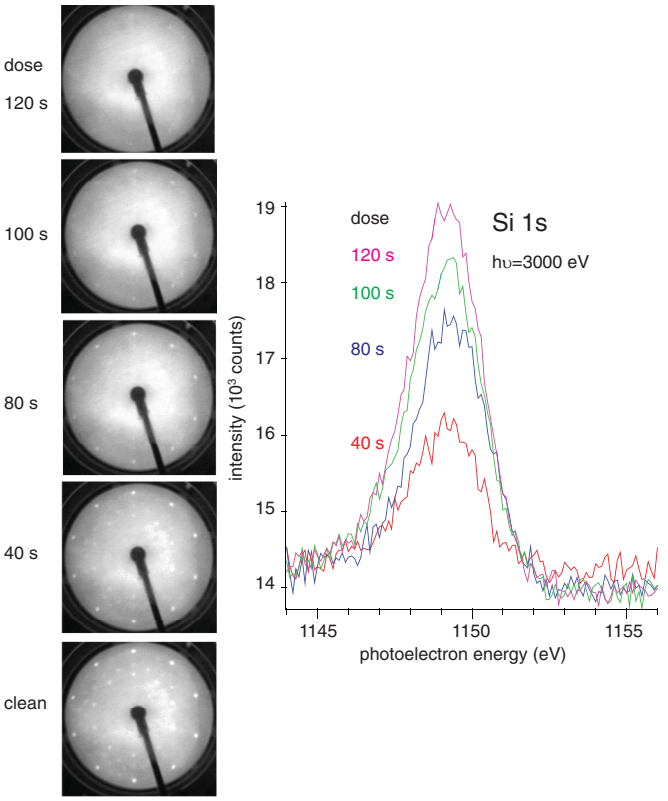

FIG. 1. (Color online) LEED patterns (left) and XPS scans (right) recorded for increasing Si dosing times. The XPS scans are consistent with a linear increase in the coverage with dosing time. The disappearance of the LEED spots for dosing time ∼120 s is identified as one complete layer of Si.

10-fold symmetric LEED pattern. NIXSW measurements were recorded from the surface with an estimated coverage of ∼0.2 ML of Si, deposited from a Knudsen cell, with the sample at room temperature. This is the same preparation procedure as in the STM study of this system [7], and was reproduced in order to ensure that the results of this earlier characterization of the surface may be expected to be relevant to our investigation. Figure 1 shows LEED patterns and XPS spectra as a function of dosing time. The earlier study [7] identified the disappearance of the LEED spots (at about 120 s in this experiment) with a coverage of 0.75, as determined by STM and Auger electron spectroscopy. Since the STM thresholding method for coverage measurement tends to overestimate submonolayer coverages, we estimate that a 40 s dose in our experiments corresponds to a coverage of ∼0.2 ML, where 1 ML corresponds to one complete layer.

The NIXSW experiments were performed using beamline 4.2 of the Daresbury Laboratory's Synchrotron Radiation Source. This beamline was fitted with double crystal [InSb(111)] monochromator and a surface science end chamber. A concentric hemispherical analyzer (at 40° to the incident photon beam in the horizontal plane) was used to measure the photoelectron energy spectra. The x-ray absorption at the adsorbed Si atoms was monitored by measuring the intensity of the Si 1*s* photoemission, while the intensity of the electron emission background at a slightly higher energy provided a measure of the variation of the bulk absorption through the NIXSW photon energy scans. This background NIXSW profile was used to provide the absolute energy reference for analysis of the Si NIXSW absorption profiles.

The NIXSW data using normal incidence to the (truly periodic) (00004) scatterer planes parallel to the surface (at a nominal photon energy of 3053 eV), provided a measure of the Si adsorbate positions perpendicular to the surface. Following the general methodology used in studies of crystalline surfaces, additional NIXSW measurements were recorded using a scattering plane tilted relative to the surface, in order to gain information on the lateral position of the Si atoms on the surface. Specifically, NIXSW was recorded from a set of quasicrystalline scattering planes inclined at 60.4° to the surface with an average interlayer spacing of 2.03 Å, leading to a closely similar nominal Bragg energy of 3060 eV. This use of NIXSW data using scattering from the planes parallel to the surface, and from one set of planes that are canted relative to the surface, is sufficient to fully triangulate the location of absorber atoms on a crystalline surface with more than twofold rotational symmetry, as has been shown in many applications of the method [29,30].

III. RESULTS

To analyze the results of the NIXSW measurements from this quasicrystal, we have made use of a 200 Å × 200 Å × 8.147 Å structural model (referred to hereafter as the 200 Å model) fitted to intensities measured in an x-ray diffraction study of the basic Co-rich Al-Co-Ni quasicrystal [42,44]. In this model structure, no distinction is made between Co and Ni atoms due to their similar scattering properties, and therefore we refer to these collectively as transition metal (TM) atoms. The interplanar distances and angles differ slightly for the quasicrystal and the 200 Å model (and also for the "W model"—see Sec. IV). The relevant parameters are given in Table I.

Although the quasicrystal structure is not periodic in the *x* and *y* directions, the analysis here treats the 200 Å model as a periodically repeating unit cell. Since the quasicrystal structure is truly periodic perpendicular to the surface, this has no consequence for finding the height of the Si atoms above those periodic planes. It does have consequences for other directions, however. While the quasicrystal surface used in

TABLE I. Parameters for the Al-Co-Ni quasicrystal and the two periodic structure models used in this analysis. θ refers to the angle between the $(0\bar{1}\bar{1}01)$ and (00004) planes.

Parameter	Quasicrystal	200 Å model	W model
d (00004)	2.04 Å	2.037 Å	2.043 Å
d $(0\bar{1}\bar{1}01)$	2.02 Å	2.032 Å	2.039 Å
θ $(0\bar{1}\bar{1}01)$	60.4°	60.078°	60.007°
Cell parameters	a	b	c
200 Å model	200 Å	200 Å	8.147 Å
W model	39.688 Å	23.392 Å	8.158 Å

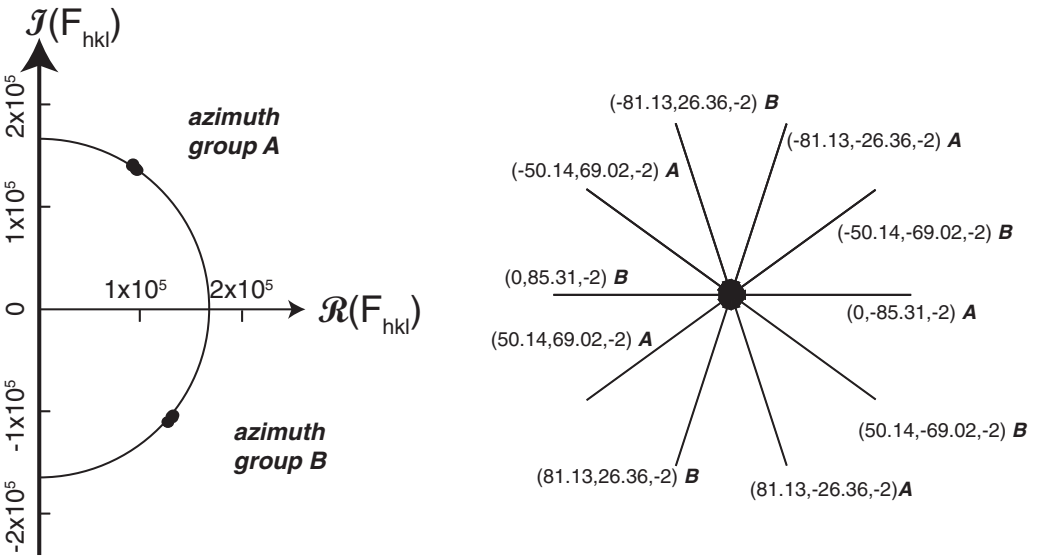

FIG. 2. Argand diagram (left) showing the complex structure factors calculated for the 200 Å × 200 Å model of the bulk quasicrystal for the two nominally fivefold equivalent sets of reflections, in 10 different azimuthal directions. The values fall into one of two groups, A and B, each comprising five directions separated by intervals of 144°, that reflect the local fivefold symmetry of the reference point. On the right are shown the different azimuthal incidence directions corresponding to the 10 different indexed reflections.

the experiment has fivefold symmetry, any periodic structure, even one artificially imposed such as this one, cannot have fivefold symmetry. The degree of fivefoldedness of the 200 Å model is evident in the complex structure factors used in the analysis here, calculated for the set of $(0\bar{1}\bar{1}01)$ quasicrystalline scattering planes used in the NIXSW experiment (Fig. 2). Of course the actual structure factor values depend on the choice of the origin of the lateral coordinates used in their calculation; for a crystalline solid this is taken to be the corner of the unit cell, a position generally corresponding to a point of high symmetry in the crystal. In the present case of our quasicrystal we chose this reference to be a point of local fivefold symmetry, leading to close bunching of the structure factors into two values corresponding to the (0, 85.31, −2) reflection and its nominal fivefold counterparts, and the (0, −85.31, −2) reflection and its nominal fivefold counterparts. These values fall on the same circle in the Argand diagram and thus have essentially the same modulus of the structure factor but differ in phase by $\sim\pi/2$, consistent with the 10-fold symmetry observed in x-ray diffraction and indicative of a structure having $\bar{10}$ inversion symmetry [42]. Note that the Miller indices for the reflections used here have noninteger values because they are indexed relative to the 200 Å unit cell, an arbitrary length not related to the actual atomic structure of the model, which has an average interplanar spacing in this direction of 2.032 Å.

Our NIXSW experiment was performed using just one azimuthal direction that must belong to either azimuthal group A or azimuthal group B, but it is not possible to tell which on the basis of our LEED pattern (nor would it be possible from a similar x-ray diffraction pattern), since the intensities are the same for both sets of reflections. It is also not possible to distinguish these directions from NIXSW measurements of absorption in the bulk of the crystal, as described in Sec. III B. However, the analysis procedure that we have developed here does allow this distinction to be made.

A. NIXSW from the periodic planes parallel to the surface

Relative to the unit cell of the model, the NIXSW measurement exploiting the periodic scattering planes parallel to the surface corresponds to the (004) reflection; in the five-index scheme used for the quasicrystal, it is the (00004) reflection. The experimental NIXSW profiles obtained from these scattering planes at both the adsorbed Si atoms (as monitored by the intensity of the Si 1*s* photoemission) and in the bulk (obtained from the intensity of inelastically scattered electron background at an energy a few eV above the Si 1*s* peak), as a function of the photon energy that is scanned through the (00004) reflection condition, is shown in Fig. 3. Also shown are theoretical fits to the data using the standard procedure used in earlier studies of periodic crystal surfaces [29,30]. Note that the use of the bulk absorption profile to provide the absolute energy reference requires that the bulk structure, relative to the NIXSW scattering planes, is known, as is the case in the present system. The known structure strongly constrains acceptable values of CP (but not CF) in the fitting of the bulk profile. The substrate absorption signal shows a good signal-to-noise level and a profile characteristic of most absorbing atoms lying on the scattering planes. Specifically, background measurements (both above the Si 1*s* peak, but also at other energies close to Al, Ni, and Co Auger electron emission peaks) gave a CP value of 0.05 ± 0.03, the precision being based on the scatter of five separate measurements; this is slightly larger than the expected value of 0.00. NIXSW profiles recorded using these substrate Auger emission peaks yielded closely similar values. We therefore infer that the consistent offset is most probably due to a small systematic error arising in the calculation of the (004) structure factor in the (fully periodic) structural model of the quasicrystalline bulk. The CF value found for these absorption profiles was 0.82 ± 0.05; this value is very slightly lower than is typical of an elemental crystalline solid, but to be expected here due to the buckling of

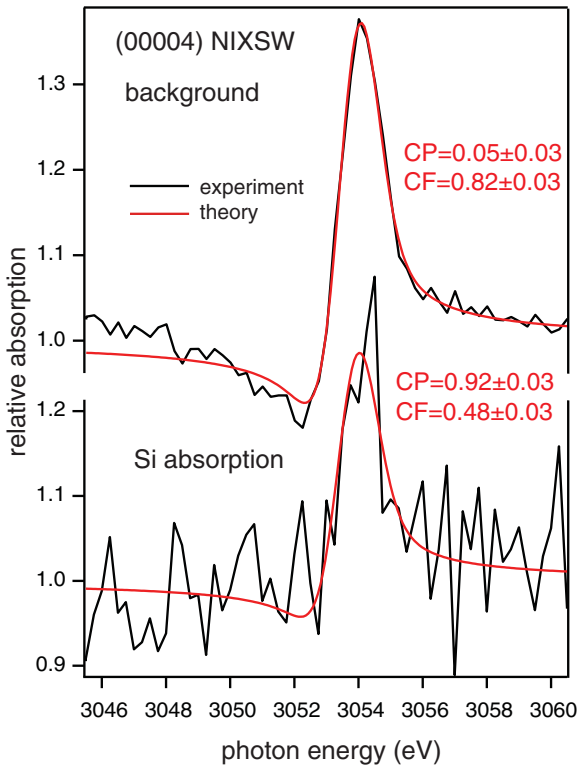

FIG. 3. (Color online) Comparison of one pair of experimental (00004) NIXSW absorption profiles from the substrate and from the adsorbed Si atoms with the best-fit theoretical calculations for the (004) profiles from the model described at the beginning of Sec. III.

the layers. Not surprisingly, the NIXSW profile from the much smaller number of adsorbed Si atoms shows substantially worse statistics (as seen in Fig. 3), but can be fitted with a CP value of 0.13 ± 0.03 less than that found for the substrate absorption profiles. This fitting of the NIXSW absorption profile monitored by the Si $1s$ photoemission signal takes account of the quadrupolar backward-forward asymmetry of the photoemission signal (which renders the photoemission and true absorption profiles inequivalent) by inclusion of the asymmetry parameter Q, for which a value of 0.15 was taken from previous calibration experiments that were also found to be consistent with theoretical calculations [45]. The determined CP value indicates that the Si atoms have an average height above the outermost bulk-extended substrate layer in units of the periodicity of the scattering planes (2.04 Å) of $(1.00 - 0.13) = 0.87$, giving a value of 1.77 ± 0.05 Å for this height. In the absence of any relaxation of the outermost substrate layer spacings, this value also corresponds to the true average height above the outermost substrate layer. The value of the CF found to fit the Si absorption profiles was 0.48 ± 0.05, significantly lower than that of the substrate; this suggests that there is a significant range of different heights occupied. The CP and CF values obtained in this analysis are summarized in Fig. 3.

B. NIXSW from the quasiperiodic planes inclined to the surface

NIXSW experiments conducted using scattering planes inclined to the surface allow one to determine the location of adsorbed atoms relative to these planes, and as the perpendicular to these planes has a component parallel to the surface, information on the lateral position of the atoms can be extracted. In order to maximize the signal we chose the $(0\bar{1}\bar{1}01)$ planes, which have the second-highest scattering amplitudes for Al-Co-Ni, after the (00004) planes [46]. For the quasicrystal, there are five reflections that are symmetrically identical to those from the $(0\bar{1}\bar{1}01)$ planes, all tilted 60.4° from (00004) planes and having an interlayer spacing of 2.02 Å (see Table I) [42,46]. This is the geometry used in the experiment. The corresponding directions in the 200 Å model structure are those that have angles of 60.08° relative to the (00004) direction with an interplanar spacing of 2.03 Å. The Miller indices for these planes, relative to the 200 Å × 200 Å × 8.147 Å unit cell, are $(0, \pm 85.31, -2)$, $(\pm 50.14, \pm 69.02, -2)$, and $(\pm 81.13, \pm 26.36, -2)$, as discussed above (see also Fig. 2).

Figure 4 shows (a) top and (b) side views of sections of the 200 Å model. Superimposed on the side view are lines representing the tilted high-density $(0\bar{1}\bar{1}01)$ planes. Although there is no true periodicity in this structure, the atoms are arranged such as to reflect an average 2.03 Å periodicity for

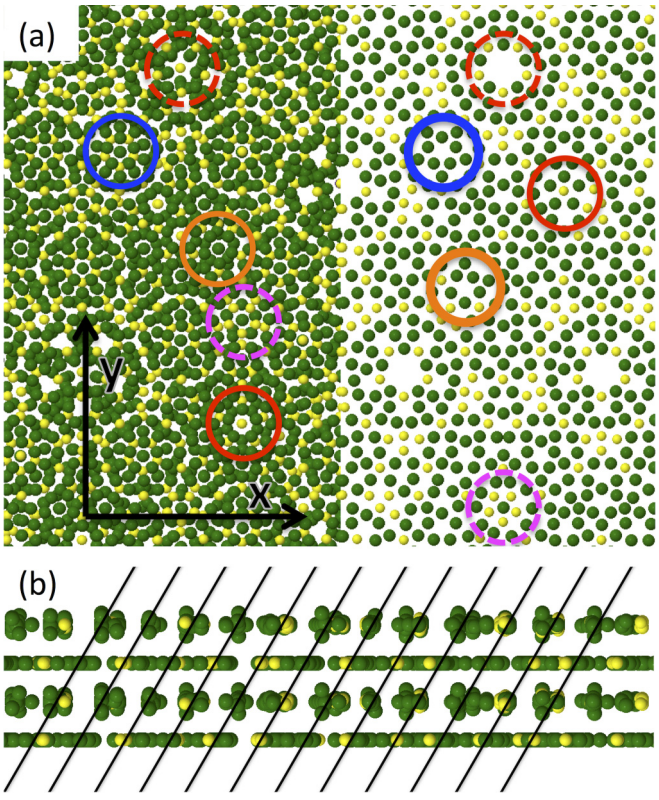

FIG. 4. (Color online) (a) Plan view of a 120 Å × 100 Å section of the structure model used in this work. The left side shows the four-layer structure, the right side shows just the top layer. Al (TM) atoms are denoted by green (yellow). The circles indicate examples of sites having local fivefold symmetry, their colors indicate equivalent sites on both sides of the drawing. (b) Side view (along the x direction) of a 35 Å wide section of the same model. The superimposed lines, inclined at 60.08° to the surface, and with a spacing of 2.03 Å, correspond to the orientation and periodicity of the scatterer planes that create the standing waves used to investigate the lateral location of atoms at the surface.

these planes, as is seen rather clearly in Fig. 4(b). In the case of a periodic crystal surface, the lateral position of adsorbed atoms typically is determined relative to the same atom in the unit cell that is used as the reference site in the calculation of the structure factor for the associated Bragg reflection. Because this location is repeated periodically in the surface, it is only necessary to locate the lateral position within the surface unit mesh. On a quasicrystal surface, however, there is no such lateral periodicity, and this simplicity is lost. However, the same problem of a lack of true periodicity underlies any diffraction or standing wave creation in a quasicrystal, and it is well established that meaningful information can be extracted on the bulk structure of quasicrystals from these methods [32,34–36]. We describe here how similar information may be extracted from NIXSW studies of the quasicrystal surface.

In the standard NISXW analysis procedure, as used for the interpretation of the experimental data of Fig. 3, the theoretical profile calculated using a single structure factor is fitted to the experiment using two adjustable parameters, the CF and the CP. These provide the key structural information, relative to the planes that pass through the reference point used to calculate the structure factor. This procedure, however, relies on the input of a single structure factor that is valid for all symmetrically equivalent directions of incidence, a situation that does not generally pertain in a study of a quasicrystal surface. In fact in the present case we have managed to identify a local fivefold symmetry site that does lead to very closely similar structure factor values for each of the two groups of symmetrically equivalent azimuths (see Fig. 2). It would therefore be possible to extract CP and CF values corresponding to the two alternative azimuthal groups, one of which must correspond to the conditions of our experiment; these could therefore be compared with alternative structural models to try to find a self-consistent solution. In general, however, it appears that a reference site cannot be identified that leads to such closely clustered structure factors (see Sec. IV). We therefore adopt an analysis approach that is more generally applicable. Specifically, in order to interpret the NIXSW data here we simulate each of the absorption profiles for particular adsorbate structure models, and then compare these simulations with the results of the experiment. In effect, the relatively direct structure determination of the standard approach is replaced by a trial-and-error approach, which is the norm for most other surface structural techniques.

We first explore this model-dependent simulation approach to the NIXSW from the bulk crystal. This approach was also used by Jach *et al.* [34] to rationalize their study of bulk NIXSW in an experiment performed at normal incidence to the surface of a quasicrystal. Here we simulated the bulk absorption that is to be expected for incidence in the two symmetrically inequivalent azimuthal directions. Figure 5 shows the experimental substrate absorption profiles, obtained from a measurement of the yield in the background inelastically scattered electron emission, along with simulated profiles, based on the known 200 Å × 200 Å structural model, for the two alternative azimuthal groups identified in Fig. 2. The calculated profiles are based on the assumption that all bulk atoms (Al and TM) contribute equally to the absorption. Insofar as the measured photoelectron background is proportional

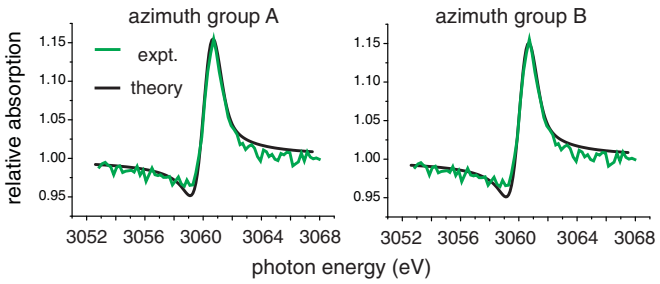

FIG. 5. (Color online) Experimental and calculated NIXSW substrate absorption profiles. The experimental profile was recorded from the $Al_{72}Ni_{11}Co_{17}$ quasicrystal surface from scattering planes inclined at 60.4° to the surface with a spacing of 2.02 Å. The results of the experiment are compared with simulations for incidence in each of the two alternative azimuthal groups.

to the total absorption, this assumption is broadly consistent with published mass absorption coefficient values at a photon energy of 3 keV of 705 cm^2/g for Ni and 780 cm^2/g for Al [47]. The good agreement between experiment and theory reinforces this view.

An important result of the comparisons in Fig. 5 is that the calculated profiles for the two azimuths are identical in spite of the different structure factor phases. At first sight this seems surprising, because NISXW is sensitive to the phase of the x-ray wavefield within the crystal, but the equivalence of the two NIXSW results simply indicates that the x-ray scattering is identical in phase as well as amplitude relative to the dense atomic absorber and scatterer planes, and not to the position of these planes relative to some arbitrary fixed reference point in the crystal. As a result the bulk standing wave measurements do not tell us which azimuth was measured in the experiment; it has been shown to be possible to resolve this distinction using multiple-beam x-ray diffraction [48].

In order to simulate the Si NIXSW absorption profile from these canted planes we must identify possible structural models for the adsorbed atoms. An earlier STM study of this surface appeared to show six-atom pentagons of Si at a low Si coverage [7], each consisting of a ring of five atoms plus a sixth one at the center. Pentagons having two azimuthal orientations, rotated by 36° relative to each other, were observed, and their spatial distribution was quasiperiodic, consistent with adsorption in specific sites. Simulations of the Si NIXSW absorption profile were therefore performed for structural models comprising six-atom pentagonal clusters of Si in locations centered on points of fivefold symmetry on the model of the underlying surface, at an average height of 1.77 Å, the value indicated by the (00004) NIXSW analysis. Some examples of different fivefold sites are indicated in Fig. 4(a). Figure 6 is a similar diagram of a smaller area of the surface that identifies fivefold sites having hollows at their centers. These hollow sites occur in two orientations on the surface that we label RSU (right-side up) and USD (upside down) in Fig. 6; on both figures these sites are indicated with blue and orange circles, respectively. Two rather different Si pentagon models with different diameters can be considered at each of these sites. Examples of the smaller pentagon model, corresponding to an RSU Si pentagon on a USD site (labeled

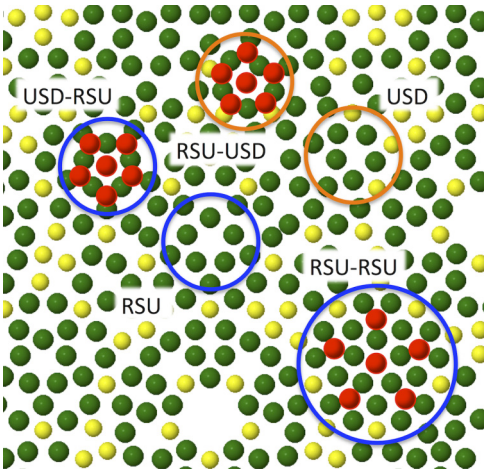

FIG. 6. (Color online) Plan view of just the top layer of the model shown in Fig. 4(a), with six-atom pentagons of Si atoms (red) superimposed in possible locations having local fivefold symmetry. Al, TM, and Si atoms are denoted as green, yellow, and red, respectively. RSU and USD indicate right-side up and upside down pentagonal sites (blue and orange circles, respectively). Si pentagons are shown in such sites; the nomenclature RSU-USD, for example, refers to an RSU Si pentagon in a USD site. The larger blue circle identifies an example of an expanded Si pentagon that has its outer Si atoms in larger hollows.

RSU-USD), and a USD pentagon on an RSU site (USD-RSU), are shown on the upper part of Fig. 6. In this model the central Si atom occupies the hollow at the fivefold symmetric center, while the five Si rim atoms are threefold coordinated to the underlying substrate atoms. If these smaller Si pentagons are rotated by 36° to a RSU-RSU or USD-USD combination the rim atoms then occupy near-atop sites relative to the underlying substrate atoms; this version of the small pentagon model can be rejected as incompatible with the results of the (00004) NIXSW, because for reasonable Al-Si (or TM-Si) bond lengths of about 2.5 Å, the layer spacing must differ considerably from the required value of 1.77 Å. Evidently this height constraint rules out all models in which most Si atoms are close to being on top of substrate atoms.

By contrast in the larger pentagon model, with the pentagon orientation having the same orientation as the substrate atoms that define the site (i.e., USD-USD and RSU-RSU—an example is shown in the lower part of Fig. 5), the Si rim atoms lie in fivefold coordinated hollow sites, while the RSU-USD and USD-RSU combinations place the rim atoms in near-atop sites. In fact neither of these rotational combinations for the large pentagon model is consistent with the average height of the Si layer being consistent with the 1.77 Å value obtained from the (00004) NIXSW. For the RSU-USD and USD-RSU combination the Si rim atoms are much too high, while in the RSU-RSU and USD-USD combinations *all* the Si atoms should lie at much smaller layer spacings of ∼1.3 Å.

The quasicrystal surface also contains a number of TM or Al centered pentagons (see Fig. 4). However, for the small Si pentagons like those shown in the upper part of Fig. 6, the average height of the Si will be too high for any orientation of the Si pentagon in such a site. We also note that most of the atom-centered pentagonal sites evident in Fig. 6 are too rare on the surface to account for the observed density of Si pentagons observed in STM images [7]. Although the distance between the outer Si atoms in the chosen clusters is about 3.0 Å, considerably smaller than the 4.2 Å derived from the STM images [7], a similar discrepancy was noted for the STM measurements of 10-atom Pb pentagonal clusters on Al-Pd-Mn [6] and attributed to cluster distortion during scanning due to tip-adatom forces. To summarize, the only combinations of Si pentagon and site that are consistent with the constraints given by the (00004) NISXW and the STM data are those represented by the smaller Si pentagons in Fig. 6. However, we will demonstrate that even without these constraints, the NISXW from the canted planes allows us to distinguish the different sites with local fivefold symmetry shown in Fig. 4.

Simulation of the NIXSW profiles expected from absorption by the Si atoms in these pentagons is straightforward, using the standard expression for absorption at a specific layer spacing of the absorber relative to the set of scatterer planes passing through the reference atom used to calculate the structure factors. This expression, modified to account for the fact that the NIXSW is detected by the Si 1*s* photoemission signal, which has a quadrupolar backward/forward asymmetry, is given, for example, by Lee *et al.* [45]. Before presenting the results of these simulations for the Si pentagon models, however, we first present results that address a more general issue, namely does NIXSW from these canted reflection planes reflect the local self-similarity that characterizes the quasicrystalline state?

As remarked above, on the surface of a crystalline solid, measurements of NIXSW using scattering planes canted relative to the surface provides a means of determining the location of the absorber atoms within the surface unit mesh. On a quasicrystal surface, however, there is no true periodicity and no surface unit mesh. Many similar pentagon sites exist on the surface, but their relative locations are defined by the quasicrystalline order, not by a periodic lattice, so the question is whether the NIXSW results reflect this different type of ordering. To address this question, NIXSW simulations were first performed for single Si atoms adsorbed at the hollow sites at several different fivefold-symmetric RSU and USD sites, in each case computing the results for the two different azimuthal groups.

Figure 7 shows clearly that the NIXSW simulations for adsorption at locally equivalent centers are, indeed, identical, this self-similarity reflecting the quasicrystalline character of the surface. These results also show that the simulations are quite different from the two different types of centers, and also depend strongly on which of the two fivefold sets of incidence azimuths are used. One might also ask, if the NIXSW is essentially identical for (locally equivalent) sites separated by significant distances on the surface, how sensitive are these measurements to smaller lateral displacements on the surface?

Figure 8 shows the results of calculations, for a single Si absorber atom at different lateral displacements from an RSU center, that provide an answer this question. Evidently both the shape and amplitude of the NIXSW profile change significantly with lateral displacement. Notice that all of these calculations involve an average over the five symmetrically equivalent azimuthal directions, so as the absorber atom moves

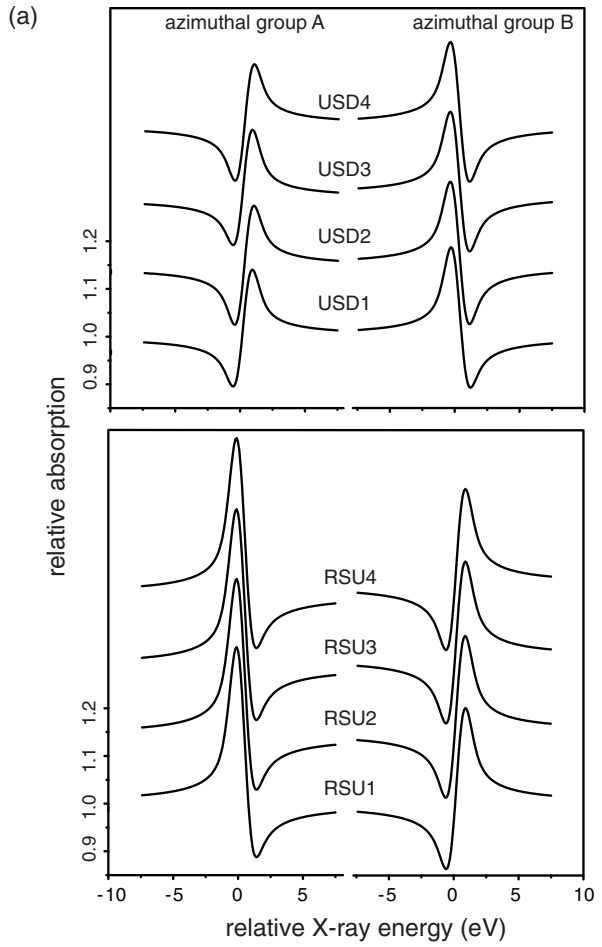

FIG. 7. (Color online) (a) NIXSW canted-plane simulations for single Si atoms at the pentagonal centers shown in the plan view of the top layer of the substrate (b), calculated for each of the two different groups of incidence azimuths.

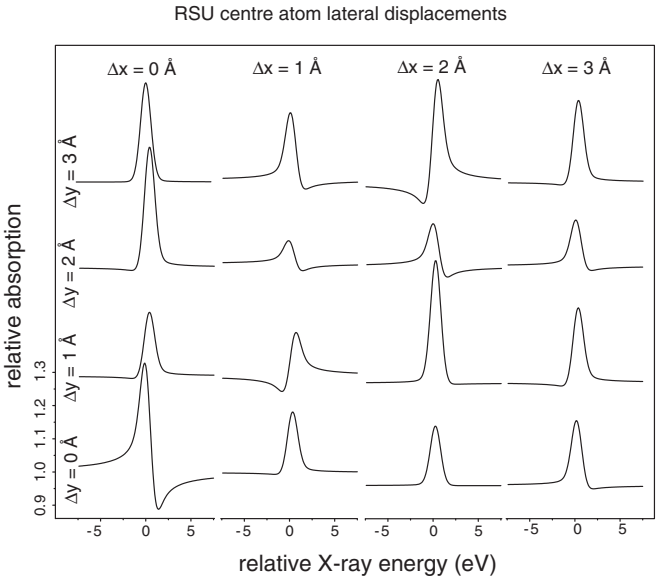

FIG. 8. NIXSW canted-plane simulations (performed in azimuthal group A) for a single Si atom located at an RSU center [as shown in Fig. 6(b)] and for different lateral displacements from this local fivefold symmetric site.

away from the most symmetric site one expects the NIXSW profile to have an increasing incoherent component. A purely incoherent profile (identical to the reflectivity profile) is (after the Gaussian broadening used to account for instrumental effects on this low-resolution beamline) essentially symmetrical with no negative excursions. Indeed, this qualitative effect can be seen in many of the simulated profiles of Fig. 8 although in fact none of them have both the shape and the amplitude that characterizes a fully incoherent absorption profile.

As shown in Fig. 9 the qualitative behavior of NISXW simulations for complete small-diameter RSU-USD and USD-RSU Si pentagons is similar to that of the center atoms alone, shown in Fig. 7; specifically, the full self-similarity property is retained, although the sensitivity to the identity of the site and the azimuthal direction is reduced, presumably due to the introduction of the pentagon rim atoms that occupy lower symmetry sites.

In Fig. 10 we return briefly to the question of whether we can distinguish the alternative local fivefold sites even if the constraints imposed by Si-substrate bond lengths are ignored. Specifically, the results of calculations are shown for single Si atoms adsorbed at the three alternative locally fivefold symmetric sites, but with a layer spacing [compatible with the (00004) NIXSW results] equal to that used for the RSU site calculations of Fig. 7. This layer spacing is actually unphysically large for the sites identified by the dashed red circles of Fig. 4, and unphysically small for the sites identified by the dashed magenta and solid red circles of Fig. 4, but it is clear that these sites lead to very different NIXSW profiles from those of the RSU and USD sites shown in Fig. 7.

Finally, Fig. 11 shows a comparison of the experimental NIXSW profile obtained from the Si 1*s* photoemission signal, recorded from the canted scatterer planes, with the results of simulations in each of the two azimuthal groups for the structural model based on equal occupancy of the small diameter USD-RSU and USD-RSU Si pentagons on the surface. In each of these pentagonal structures the Si atoms

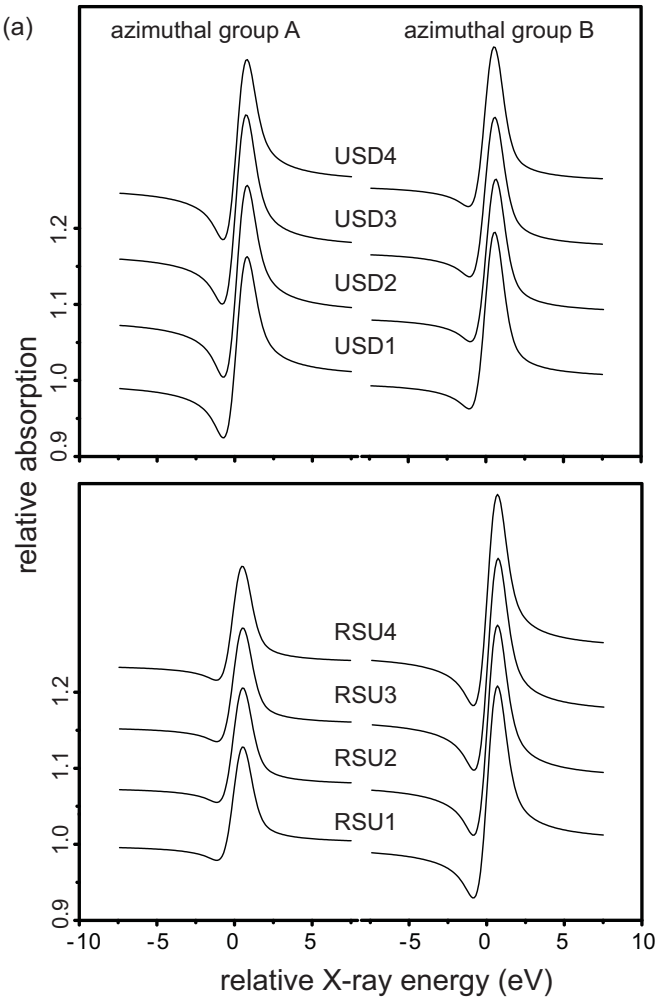

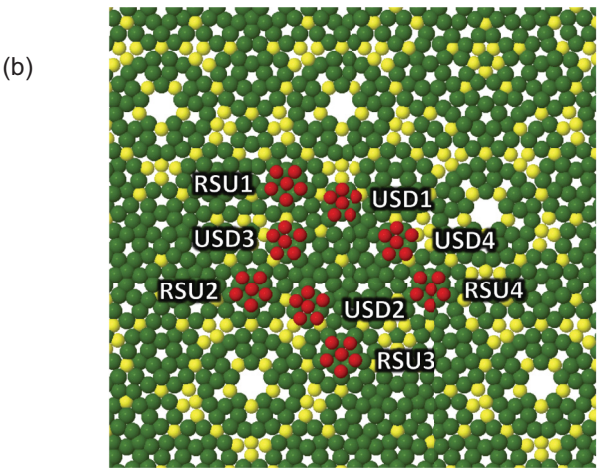

FIG. 9. (Color online) (a) NIXSW canted-plane simulations for complete Si pentagonal clusters shown in the plan view of the surface (b), calculated for each of the two different groups of incidence azimuths. The RSU/USD labeling relates to the orientation of the sites as described in the text.

were first relaxed onto the rigid model of the surface to ensure Si-Al bond lengths close to 2.5 Å. Figure 11 shows quite good agreement between the experimental and simulated NIXSW profiles for both azimuthal groups, but both the exact energy

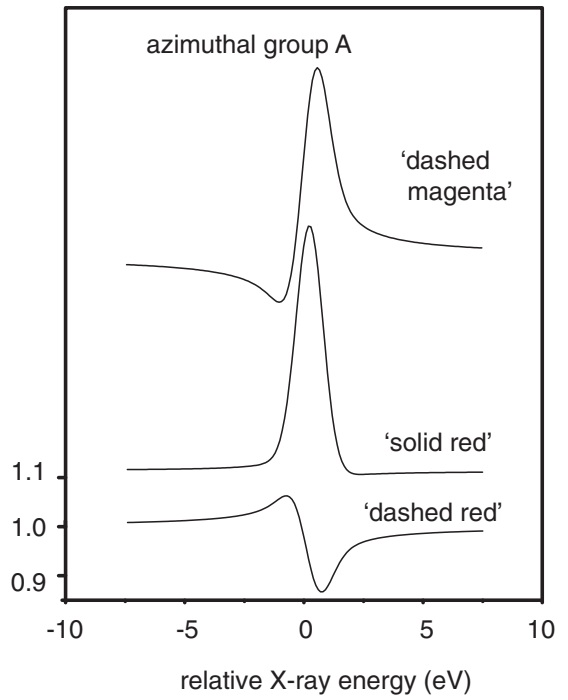

FIG. 10. NIXSW canted-plane simulations (performed in azimuthal group A) for a single Si atom located at the three alternative locally fivefold symmetric sites shown in Fig. 4 adsorbed at that same layer spacing as for the RSU centers (cf. Fig. 7).

of the peak and the modulation amplitude are significantly better for the simulations calculated for azimuthal group B. We therefore conclude that this structural model is consistent with the NIXSW data, that it is the only model we have identified that fulfills the requirements of reasonable bond lengths and occupation of locally equivalent sites on this quasicrystal surface, and that the experiment was performed with incidence in one of the azimuthal group B directions.

IV. USE OF APPROXIMANT STRUCTURES

While our investigation of the specific quasicrystal investigated here demonstrates the viability of the NIXSW technique

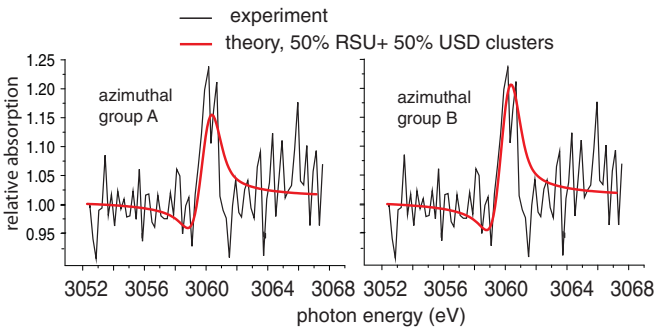

FIG. 11. (Color online) Comparison of the experimental NIXSW data from the Si 1*s* photoemission signal recorded from the canted scatterer planes with the results of simulations in each of the two azimuthal groups for the structural model based on equal occupancy of the small diameter USD-RSU and RSU-USD Si pentagons on the surface.

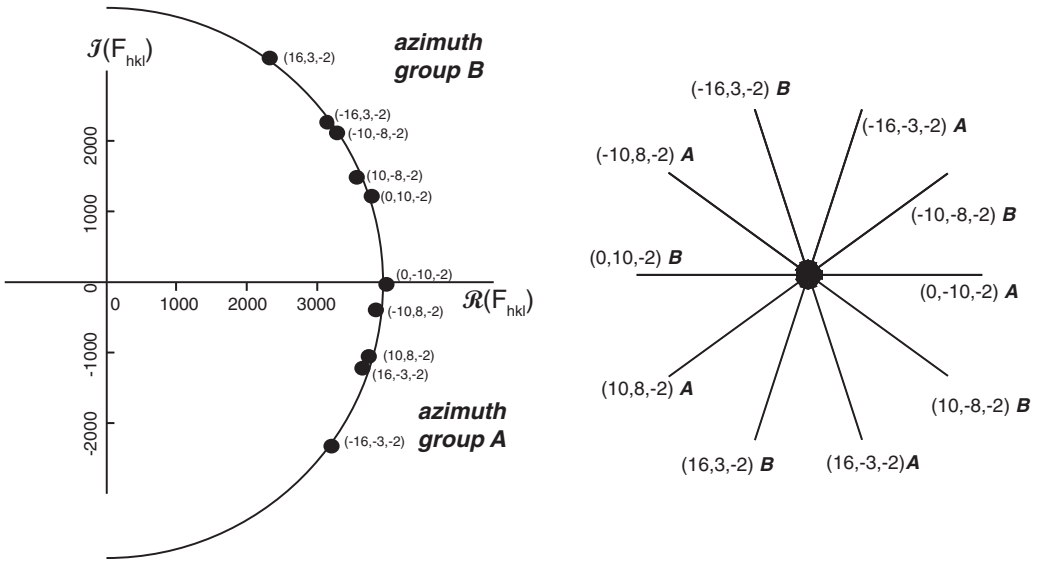

FIG. 12. Structure factor diagram similar to that of Fig. 1, but for the W approximant. On the left is an Argand diagram showing the complex structure factors for the 10 different azimuthal directions. On the right are shown the different azimuthal incidence directions corresponding to the 10 different indexed reflections.

to determine adsorbate structures on quasicrystal surfaces, there is no doubt that this analysis has benefitted significantly from the availability of the large 200 Å × 200 Å "unit mesh" structure determination of the bulk structure. Many other quasicrystal surfaces of potential interest do not have such detailed bulk structure determinations. One possible way to overcome this limitation is through the use of quasicrystalline approximants—periodic structures that are close analogs of quasicrystals. In the case of the decagonal $Al_{72}Co_{17}Ni_{11}$ quasicrystal studied here there are a number of closely related crystalline approximants, and we have therefore explored the extent to which an analysis of our experimental data may be conducted using one of these approximants.

In order to test this idea we have used the W approximant with a bulk unit cell of dimensions 39.668 Å × 23.392 Å × 8.158 Å [49]. Of course, for our system in which there is true periodicity along the [00001] direction, the only issue involving the quasicrystalline character of the material we have studied is how to treat the data recorded from the canted planes. We therefore repeated simulations on the W approximant model similar to those described in the previous section for the much larger quasicrystal model. Figure 12 shows the calculated structure factors for the 10 different incident directions and the associated reflection indices. The clustering of the structure factor values for the two groups of fivefold symmetric directions is much weaker than that shown in Fig. 2 for the 200 Å × 200 Å model, an effect that seems to be associated with the fact that this periodic structure with a moderately large unit cell cannot have a high degree of fivefold symmetry. Structure factors calculated using several different reference points all failed to show the strong clustering into the two fivefold groups shown in Fig. 2.

Structural models of the favored Si pentagonal clusters that are essentially identical to those identified on the 200 Å × 200 Å model surface were then constructed and are shown in Fig. 13 on a diagram of the surface of the complete surface unit mesh of the W approximant. Also shown in Fig. 13 are the results of NIXSW simulations for a single Si atom adsorbed at the center of these four USD and four RSU sites. The results are essentially identical to those shown in Fig. 7 for the equivalent calculations on the 200 Å × 200 Å model surface. Notice that despite the reduced manifestation of the fivefold symmetry that could be achieved in our structure factor calculations, these NIXSW simulations show the self-similarity of the locally equivalent fivefold symmetry sites that are characteristic of the real quasicrystal surface. The strong similarity of these simulations to those of Fig. 6 also indicates that calculations using the W approximant may be just as effective as those conducted on the 200 Å × 200 Å model surface for identifying the structural model that is consistent with the experimental NIXSW data.

This conclusion is supported by the results of NIXSW simulations for the full pentagonal clusters at the RSUW and USDW sites shown in Fig. 14 that are fully consistent with the results of the equivalent clusters on the 200 Å × 200 Å model of the surface, shown in Fig. 9. Finally, Fig. 15 shows the comparison of the experimental NIXSW Si photoemission profile and the simulations based on a 1:1 mixture of Si pentagons on the RSUW and USDW sites. The results are closely similar to those obtained on the 200 Å × 200 Å model of the surface shown in Fig. 11 and lead to the same conclusions—namely good theory-experiment agreement and a preference for azimuthal group B.

V. DISCUSSION

So far we have focused on the specific results of the experiment we have performed on the $Al_{72}Co_{17}Ni_{11}$ surface, and the issues that arise when trying to extract structural information from NIXSW measurements performed using scattering planes with quasicrystalline periodicity, and for a complex structure. The lessons learned from this process, however, have wider implications.

As remarked in the Introduction, it has already been demonstrated that x-ray standing waves are established in

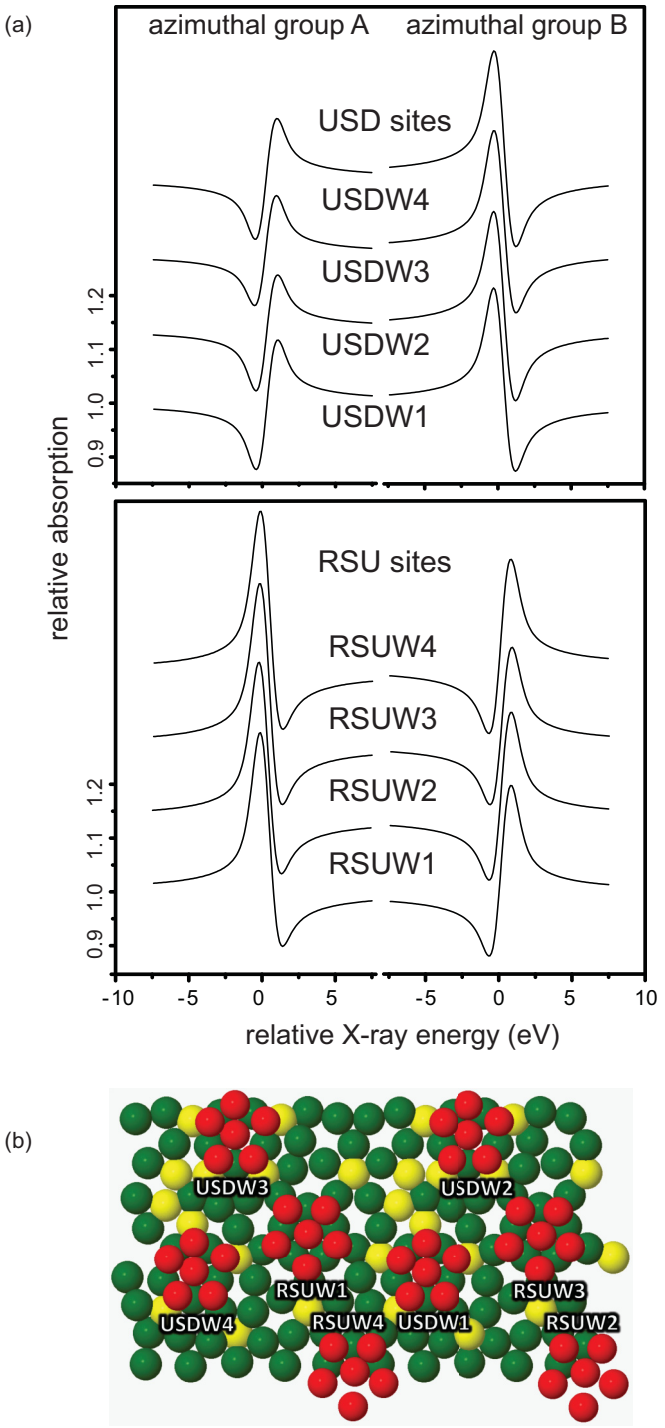

FIG. 13. (Color online) (a) NIXSW canted-plane simulations for single Si atoms at the centers of the pentagonal clusters shown in the plan view of the surface, calculated for each of the two different groups of incidence azimuths, together with (b) a schematic model of the surface and the different (small) pentagonal Si cluster sites.

quasicrystals, associated with known diffraction conditions, and that measurements of the absorption in these standing waves by atoms in the bulk, both in total and in an element-specific fashion, do yield profiles that can be fitted using nonzero CF values [33–36]. It has been shown that, even in a Fibonacci sequence of interlayer spacings, the atoms

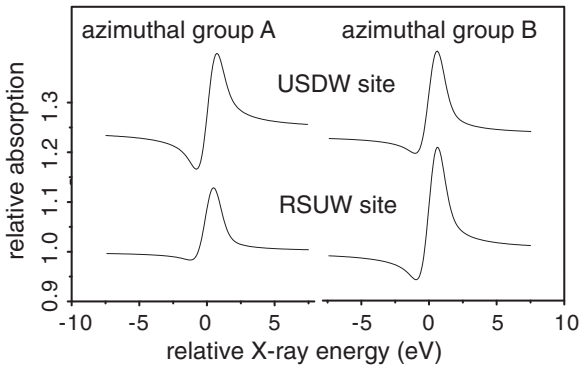

FIG. 14. NIXSW canted-plane simulations for complete Si pentagonal clusters at the RSUW1 and USDW1 sites shown in the plan view of the surface in Fig. 12, calculated for each of the two different groups of incidence azimuths.

are not randomly located relative to the periodic diffraction planes, but are clustered in such a way as to be consistent with this observation [32]. Our own measurements of the substrate NIXSW profile using the scattering planes tilted by 60.4° to the surface (Fig. 5) provide further confirmation of this fact. What had not been established previously is whether meaningful structural information can be obtained for atoms adsorbed on the surface. Although it might seem that this should follow from the observation of nonzero bulk CF profiles, the truth of this logical extension is not at all obvious.

Specifically, consider the normal case of a quasicrystal that lacks true periodicity in any direction (not the case in our experiment.) If the surface were perfectly (atomically) flat, one could conduct a NIXSW experiment using the aperiodic scattering planes parallel to the surface, and this would yield specific CP and CF values corresponding to the location of the adsorbate atoms perpendicular to the underlying quasicrystal. However, if the relationship between the location of any particular atomic plane to the phase of the standing waves is not known, one cannot transpose this information into a local adsorbate-substrate surface layer spacing. In *any* NIXSW experiment (be it from a periodic crystal or a quasicrystal) the phase of the standing wave is fixed by the location of atoms

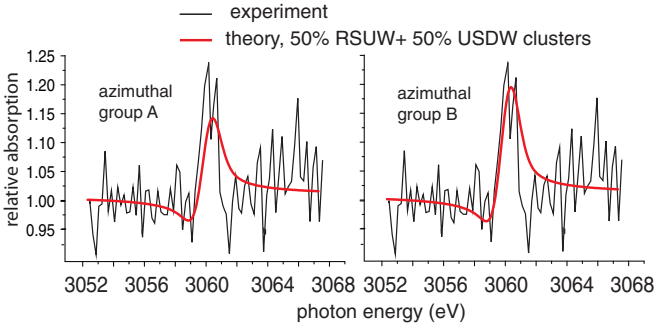

FIG. 15. (Color online) Comparison of the experimental NIXSW data from the Si 1*s* photoemission signal recorded from the canted scatterer planes with the results of simulations in each of the two azimuthal groups for the structural model based on equal occupancy of the small diameter USD-RSU and USD-RSU Si pentagons on the surface of the W approximant.

in the underlying bulk. At a periodic crystal surface we expect that the actual position of the outermost substrate layer of atoms will lie very close to that expected from an extension of the underlying periodic layers. Small surface layer spacing relaxations can occur, and in special cases even reconstruction of the outermost layers may exist, but these can usually be understood through other experiments. For a periodic crystal, knowing the location of the adsorbate atoms relative to the extended bulk planes therefore provides exactly, or almost exactly, the spacings of these adsorbate atoms relative to the atoms of the *outermost* substrate layer.

On a quasicrystal surface, however, the location of the outermost substrate atomic layer relative to the extended bulk *periodic* scattering planes is unknown, and indeed is likely to differ on different surfaces (i.e., different terminations of the bulk structure) of the same material at the same orientation, because one does not know the exact sequence of outermost substrate layer spacings. Of course, even this (apparently fruitless) experiment is idealized. A real quasicrystal surface is unlikely to be perfectly atomically flat, and will include atomic steps, and thus terraces of different heights. This will lead to a distribution of the heights of the adsorbate atoms (on different terraces, with different underlying layer spacings) above the extended reference scattering planes of the underlying bulk.

However, the problem is not quite as serious as this discussion implies, because the ordering in quasicrystals is not random, nor is the terminating layer. It has been demonstrated earlier that the locations of planes represented by a Fibonacci sequence, relative to an average periodic structure, are not random, but lie in a range of values that are described by perfectly rectangular histograms [32,50]. Thus, the structure can be described by a periodic unit cell, in which the scattering atoms are distributed primarily over a certain range of locations relative to the periodic scatterer planes. As pointed out previously [32,50], the description of the locations of the atomic planes by a range of values rather than discrete values has an effect in the diffraction analogous to the Debye-Waller attenuation due to thermal motion. We therefore expect the adsorbate NIXSW profile in such an experiment to be consistent with a finite CF value, and the associated CP value is limited in precision by the width of the histogram that describes the location of the Fibonacci planes. The width of this histogram of Fibonacci plane positions is $S/\tau \approx 0.618S$ [50], where S is the length of the short segment in the sequence, or less than half of the average interplanar spacing $\langle a \rangle = \frac{\tau L+S}{\tau+1} \approx 1.382S$ (τ is the golden ratio $=\frac{1+\sqrt{5}}{2} = 1.618\ldots$).

In addition, it has been demonstrated that in icosahedral Al-based quasicrystals such as Al-Pd-Mn and Al-Cu-Fe, the terminating layers of the fivefold surface consist of closely spaced ($\sim$0.4 Å) pairs of planes in which the outer plane is 90%–100% Al and the other plane is about 50% Al [51]. The fact that this bilayer is mostly Al and has a composite density near that of Al(111) gives it a low surface energy and thus favors it as a surface termination. Within the bulk quasicrystal, these bilayers are arranged self-similarly [52,53] as described above, and therefore their positions relative to the bulk scattering planes fall within a relatively narrow range of values.

The situation for planes tilted relative to the surface is similar. For "identical" sites on the surface (e.g., the centers of the pentagonal sites in our model structure), the positions of the atoms will fall at exactly the same location relative to the quasiperiodic planes, even if they are in different terminating layers. In our case of adatoms that are in different sites, we will have a distribution of positions relative to the planes, but this distribution reflects the structure of the model rather than the aperiodicity of the planes. If the standing waves used in the experiment have a wavelength close to the average interplanar spacing, then the precision of the experimental measurement will be defined by this same distribution. However, if the x rays used in the experiment are tuned to a higher harmonic reciprocal lattice vector of the quasicrystal, then the precision can be increased significantly (by a factor of τ for each harmonic), because the histogram profile becomes narrower for higher momentum transfer [32,50]. In principle, by measuring profiles for several harmonics in several directions, NISXW could be used to triangulate the positions of adsorbed atoms to an arbitrarily high precision, although experimental considerations of spectral resolution and absorption cross sections will undoubtedly restrict the number of possible higher-order (higher-energy) measurements. The generality of this approach depends on the availability of good structural models for the underlying quasicrystal.

VI. CONCLUSIONS

We have demonstrated that the geometries of adsorbates on quasicrystalline surfaces can be determined using NISXW. For the structure studied here, and perhaps for complex structures in general, it requires the calculation of the standing wave profiles from a model structure, rather than the direct determination of CF and CP from the measured profiles. We have demonstrated this approach for Si atoms adsorbed on the (00001) surface of the decagonal Al-Co-Ni quasicrystal. This quasicrystal is periodic in the direction perpendicular to the surface, allowing the adsorption height to be obtained using conventional methods. However, the determination of the lateral location of the adsorbed atoms requires the use of the model calculations described above. The results are consistent with the formation of six-atom pentagonal clusters of Si, which are found to reside 1.77 Å $\pm$ 0.05 Å above the surface and to occupy specific hollow sites of fivefold symmetry in such a way that maximizes the coordination of the Si atoms to the substrate.

ACKNOWLEDGMENTS

We thank Walter Steurer for the coordinates of the 200 Å quasicrystalline structure and the W approximant structure, and much useful information concerning decagonal structures. We also acknowledge useful discussions with S. M. Durbin, M. Widom, U. Grimm, J. A. Smerdon, and J. Wolny. This research was supported by NSF Grant No. DMR-0505160, A.M. received support from the DAAD-RISE program. We acknowledge the award of beam time by the Daresbury Laboratory of the CCLRC (UK Council for the Central Laboratories of the Research Councils) and the CNRS for the INCAS project (PICS05892). K.R.J.L. and A.D. would like to thank the EPSRC and the University of Nottingham for the award of studentships.

[1] Z. M. Stadnik, *Physical Properties of Quasicrystals* (Springer, Berlin, 1999), Vol. 166.

[2] J.-B. Suck, M. Schreiber, and P. Häussler, *Quasicrystals: An Introduction to Structure, Physical Properties and Applications* (Springer, Berlin, 2010), Vol. 55.

[3] J. A. Smerdon, K. M. Young, M. Lowe, S. S. Hars, T. P. Yadav, D. Hesp, V. R. Dhanak, A. P. Tsai, H. R. Sharma, and R. McGrath, Nano Lett. **14**, 1184 (2014).

[4] Z. V. Vardeny, A. Nahata, and A. Agrawal, Nat. Photon. **7**, 177 (2013).

[5] J. Ledieu, É. Gaudry, L. N. Serkovic Loli, S. A. Villaseca, M.-C. de Weerd, M. Hahne, P. Gille, Y. Grin, J.-M. Dubois, and V. Fournée, Phys. Rev. Lett. **110**, 076102 (2013).

[6] J. Ledieu, M. Krajčí, J. Hafner, L. Leung, L. H. Wearing, R. McGrath, T. A. Lograsso, D. Wu, and V. Fournée, Phys. Rev. B **79**, 165430 (2009).

[7] L. Leung, J. Ledieu, P. Unsworth, T. A. Lograsso, A. R. Ross, and R. McGrath, Surf. Sci. **600**, 4752 (2006).

[8] J. A. Smerdon, H. R. Sharma, J. Ledieu, and R. McGrath, J. Phys.: Condens. Matter **20**, 314005 (2008).

[9] V. Fournée, É. Gaudry, J. Ledieu, M. C. de Weerd, D. Wu, and T. A. Lograsso, ACS Nano **8**, 3646 (2014).

[10] M. Krajčí, J. Hafner, J. Ledieu, V. Fournée, and R. McGrath, Phys. Rev. B **82**, 085417 (2010).

[11] T. Cai, F. Shi, Z. Shen, M. Gierer, A. I. Goldman, M. J. Kramer, C. J. Jenks, T. A. Lograsso, D. W. Delaney, P. A. Thiel, and M. A. Van Hove, Surf. Sci. **495**, 19 (2001).

[12] M. Gierer, M. A. Van Hove, A. I. Goldman, Z. Shen, S.-L. Chang, C. J. Jenks, C.-M. Zhang, and P. A. Thiel, Phys. Rev. Lett. **78**, 467 (1997).

[13] M. Gierer, M. A. Van Hove, A. I. Goldman, Z. Shen, S.-L. Chang, P. J. Pinhero, C. J. Jenks, J. W. Anderegg, C.-M. Zhang, and P. A. Thiel, Phys. Rev. B **57**, 7628 (1998).

[14] N. Ferralis, K. Pussi, E. J. Cox, M. Gierer, J. Ledieu, I. R. Fisher, C. J. Jenks, M. Lindroos, R. McGrath, and R. D. Diehl, Phys. Rev. B **69**, 153404 (2004).

[15] K. Pussi, N. Ferralis, M. Mihalkovic, M. Widom, S. Curtarolo, M. Gierer, C. J. Jenks, P. Canfield, I. R. Fisher, and R. D. Diehl, Phys. Rev. B **73**, 184203 (2006).

[16] K. Pussi, M. Gierer, and R. D. Diehl, J. Phys.: Condens. Matter **21**, 474213 (2009).

[17] K. Pussi and R. D. Diehl, Z. Kristallogr. **224**, 1 (2009).

[18] M. J. Capitan, Y. Calvayrac, D. Gratias, and J. Alvarez, Phys. B: Condens. Matter **283**, 79 (2000).

[19] T. C. Q. Noakes, P. Bailey, C. F. McConville, C. R. Parkinson, M. Draxler, J. Smerdon, J. Ledieu, R. McGrath, A. R. Ross, and T. A. Lograsso, Surf. Sci. **583**, 139 (2005).

[20] J. A. Smerdon, J. Ledieu, R. McGrath, T. C. Q. Noakes, P. Bailey, M. Draxler, C. F. McConville, T. A. Lograsso, and A. R. Ross, Phys. Rev. B **74**, 035429 (2006).

[21] T. C. Q. Noakes, P. Bailey, C. F. McConville, M. Draxler, M. Walker, M. G. Brown, A. Hentz, D. P. Woodruff, T. A. Lograsso, A. R. Ross, J. A. Smerdon, L. Leung, and R. McGrath, Phys. Rev. B **82**, 195418 (2010).

[22] T. C. Q. Noakes, J. Parle, P. Nugent, H. R. Sharma, J. A. Smerdon, P. Bailey, and R. McGrath, Surf. Sci. **620**, 59 (2014).

[23] T. C. Q. Noakes, P. Bailey, M. Draxler, C. F. McConville, A. R. Ross, T. A. Lograsso, L. Leung, J. A. Smerdon, and R. McGrath, J. Phys.: Condens. Matter **18**, 5017 (2006).

[24] D. Naumovic, P. Aebi, L. Schlapbach, C. Beeli, T. A. Lograsso, and D. W. Delaney, Phys. Rev. B **60**, R16330 (1999).

[25] D. Naumovic, P. Aebi, C. Beeli, and L. Schlapbach, Surf. Sci. **433–435**, 302 (1999).

[26] D. Naumovic, P. Aebi, L. Schlapbach, C. Beeli, K. Kunze, T. A. Lograsso, and D. W. Delaney, Phys. Rev. Lett. **87**, 195506 (2001).

[27] D. Naumovic, Prog. Surf. Sci. **75**, 205 (2004).

[28] J. C. Zheng, C. H. A. Huan, A. T. S. Wee, M. A. Van Hove, C. S. Fadley, F. J. Shi, E. Rotenberg, S. R. Barman, J. J. Paggel, K. Horn, P. Ebert, and K. Urban, Phys. Rev. B **69**, 134107 (2004).

[29] D. P. Woodruff, Prog. Surf. Sci. **57**, 1 (1998).

[30] D. P. Woodruff, Rep. Prog. Phys. **68**, 743 (2005).

[31] R. D. Diehl, H. I. Li, S. Y. Su, A. Mayer, N. A. Stanisha, J. Ledieu, K. R. J. Lovelock, R. G. Jones, A. Deyko, L. H. Wearing, R. McGrath, A. Chaudhuri, and D. P. Woodruff, Phys. Rev. Lett. **113**, 106101 (2014).

[32] J. S. Chung and S. M. Durbin, Phys. Rev. B **51**, 14976 (1995).

[33] G. Schmithüsen, G. Cappello, and J. Chevrier, Ferroelectrics **250**, 289 (2001).

[34] T. Jach, Y. Zhang, R. Colella, M. de Boissieu, M. Boudard, A. I. Goldman, T. A. Lograsso, D. W. Delaney, and S. Kycia, Phys. Rev. Lett. **82**, 2904 (1999).

[35] T. Jach, Mat. Sci. Eng. **294–296**, 315 (2000).

[36] G. Cappello, F. Dechelette, G. Schmithüsen, S. Decossas, J. Chevrier, F. Comin, V. Formoso, M. de Boissieu, T. Jach, R. Colella, T. A. Lograsso, C. J. Jenks, and D. W. Delaney, Mat. Sci. Eng. **294–296**, 863 (2000).

[37] The lack of centrosymmetry in a crystal is indicative of polarity or chirality in the structure, characteristics that can also be present in quasicrystals.

[38] S. Ritsch, C. Beeli, H.-U. Nissen, T. Gödecke, M. Scheffler, and R. Lück, Philos. Mag. Lett. **78**, 67 (1998).

[39] W. Steurer and S. Deloudi, *Crystallography of Quasicrystals* (Springer, Heidelberg, 2009).

[40] A. Yamamoto, K. Kato, T. Shibuya, and S. Takeuchi, Phys. Rev. Lett. **65**, 1603 (1990).

[41] A. Strutz and W. Steurer, Philos. Mag. **87**, 2747 (2007).

[42] A. Strutz, A. Yamamoto, and W. Steurer, Phys. Rev. B **80**, 184102 (2009).

[43] I. R. Fisher, M. J. Kramer, Z. Islam, A. R. Ross, A. Kracher, T. Weiner, M. J. Sailer, A. I. Goldman, and P. C. Canfield, Philos. Mag. B **79**, 425 (1999).

[44] A. Strutz, A. Yamamoto, and W. Steurer, Phys. Rev. B **82**, 064107 (2010).

[45] J. Lee, C. Fisher, D. P. Woodruff, M. G. Roper, R. G. Jones, and B. C. C. Cowie, Surf. Sci. **494**, 166 (2001).

[46] W. Steurer and A. Cervellino, Acta Crystallogr. Sect. A **57**, 333 (2001).

[47] J. H. Hubbell and S. M. Seltzer, *Tables of X-Ray Mass Attenuation Coefficients and Mass Energy-Absorption Coefficients* (National Institute of Standards and Technology, Gaithersburg, MD, 2004).

[48] R. Eisenhower, R. Colella, and B. Grushko, Phys. Rev. B **57**, 8218 (1998).

[49] K. Sugiyama, S. Nishimura, and K. Hiraga, J. Alloys Compd. **342**, 65 (2002).

[50] J. Wolny, Acta Crystallogr. Sect. A **54**, 1014 (1998).

[51] P. A. Thiel, Annu. Rev. Phys. Chem. **59**, 129 (2008).

[52] M. Boudard, M. de Boissieu, C. Janot, J. M. Dubois, and C. Dong, Philos. Mag. Lett. **64**, 197 (1991).

[53] A. Yamamoto, H. Takakura, and A. P. Tsai, Phys. Rev. B **68**, 094201 (2003).